JOURNAL OF THE AMERICAN COLLEGE OF CARDIOLOGY VOL. 64, NO. 8, 2014

ISSN 0735-1097/$36.00
PUBLISHED BY ELSEVIER INC. http://dx.doi.org/10.1016/j.jacc.2014.05.045

ORIGINAL INVESTIGATIONS

HCN4 Mutations in Multiple Families With Bradycardia and Left Ventricular Noncompaction Cardiomyopathy

Annalisa Milano, MSc,* Alexa M.C. Vermeer, MD,† Elisabeth M. Lodder, PhD,* Julien Barc, PhD,*‡ Arie O. Verkerk, PhD,§ Alex V. Postma, PhD,§ Ivo A.C. van der Bilt, MD,* Marieke J.H. Baars, MD, PhD,† Paul L. van Haelst, MD, PhD,‖ Kadir Caliskan, MD,¶ Yvonne M. Hoedemaekers, MD, PhD,# Solena Le Scouarnec, PhD,**††‡‡ Richard Redon, PhD,**††‡‡§§ Yigal M. Pinto, MD, PhD,* Imke Christiaans, MD, PhD,† Arthur A. Wilde, MD, PhD,* Connie R. Bezzina, PhD*

ABSTRACT

BACKGROUND Familial forms of primary sinus bradycardia have sometimes been attributed to mutations in *HCN4*, *SCN5A*, and *ANK2*. In these studies, no structural cardiac alterations were reported in mutation carriers. However, a cluster of reports in the literature describe patients presenting with sinus bradycardia in association with left ventricular noncompaction cardiomyopathy (LVNC), pointing to a shared genetic cause.

OBJECTIVES This study sought to identify the genetic defect underlying the combined clinical presentation of bradycardia and LVNC, hypothesizing that these 2 clinical abnormalities have a common genetic cause.

METHODS Exome sequencing was carried out in 2 cousins from the index family that were affected by the combined bradycardia–LVNC phenotype; shared variants thus identified were subsequently overlaid with the chromosomal regions shared among 5 affected family members that were identified using single nucleotide polymorphism array analysis.

RESULTS The combined linkage analysis and exome sequencing in the index family identified 11 novel variants shared among the 2 affected cousins. One of these, p.Gly482Arg in HCN4, segregated with the combined bradycardia and LVNC phenotype in the entire family. Subsequent screening of *HCN4* in 3 additional families with the same clinical combination of bradycardia and LVNC identified *HCN4* mutations in each. In electrophysiological studies, all found *HCN4* mutations showed a more negative voltage dependence of activation, consistent with the observed bradycardia.

CONCLUSIONS Although mutations in *HCN4* have been previously linked to bradycardia, our study provides the first evidence to our knowledge that mutations in this ion channel gene also may be associated with structural abnormalities of the myocardium. (J Am Coll Cardiol 2014;64:745–56) © 2014 by the American College of Cardiology Foundation.

From the *Department of Clinical and Experimental Cardiology, Academic Medical Center, Amsterdam, the Netherlands; †Department of Clinical Genetics, Academic Medical Center, Amsterdam, the Netherlands; ‡ICIN-Netherlands Heart Institute, Utrecht, the Netherlands; §Department of Anatomy, Embryology and Physiology, Academic Medical Center, Amsterdam, the Netherlands; ‖Department of Cardiology, Antonius Hospital, Sneek, the Netherlands; ¶Department of Cardiology, Erasmus MC, Rotterdam, the Netherlands; #Department of Genetics, University Medical Centre Groningen, Groningen, the Netherlands; **Institut National de la Santé et de la Recherche Médicale (INSERM) Unité Mixte de Recherche (UMR) 1087, L'Institut du Thorax, Nantes, France; ††Centre National de la Recherche Scientifique (CNRS) UMR 6291, Nantes, France; ‡‡Université de Nantes, Nantes, France; and the §§Centre Hospitalier Universitaire (CHU) Nantes, L'Institut du Thorax, Service de Cardiologie, Nantes, France. The project was funded by the Netherlands CardioVascular Research Initiative (Dutch Heart Foundation, Dutch Federation of University Medical Centres, the Netherlands Organisation for Health Research and Development, and the Royal Netherlands Academy of Sciences) PREDICT project. This work was supported by the Netherlands Heart Foundation (2009B066) and the Netherlands Heart Institute (ICIN, 038.08). The authors have reported that they

ABBREVIATIONS AND ACRONYMS

cDNA = complementary deoxyribonucleic acid

CHO = Chinese hamster ovary

ECG = electrocardiogram

GoNL = Genome of the Netherlands

ICD = implantable cardioverter-defibrillator

LVNC = left ventricular noncompaction cardiomyopathy

NHLBI = National Heart, Lung, and Blood Institute

OHCA = out-of-hospital cardiac arrest

SAN = sinoatrial node

SNP = single nucleotide polymorphism

WT = wild-type

Sinus bradycardia, arbitrarily defined as a heart rate lower than 60 beats/min, can occur at any age and in a variety of cardiac diseases (1). Although familial forms of primary sinus bradycardia are recognized, they have been attributed to mutations in *HCN4* (2–4), *SCN5A* (5,6), and *ANK2* (7). In these studies, no structural cardiac alterations were reported in mutation carriers. However, a cluster of reports in the literature describe patients presenting with sinus bradycardia in association with left ventricular noncompaction cardiomyopathy (LVNC) (8–11), raising the possibility that these 2 defects could have a common cause.

SEE PAGE 768

LVNC is an increasingly recognized cardiomyopathy characterized by a noncompacted left ventricular myocardial layer with numerous trabeculations and deep intertrabecular recesses (12,13). These clinical manifestations may be highly variable. LVNC may occur in isolation; however, besides sinus bradycardia, it may present together with structural congenital heart defects, neuromuscular disorders, or mitral valve abnormalities (13,14). LVNC may be associated with heart failure, (potentially) lethal arrhythmias, and systemic embolic events. It may be sporadic or familial, and thus far, has mainly been associated with mutations in genes encoding sarcomere proteins (*TMP1*, *MYH7*, *ACTC1*, *TNNT2*, and *MYBPC3*) (10,15–17), although mutations in other genes have also been reported: *TAZ* (18), *DTNA* (19), *LDB3* (20), *TNNI3*, *PLN* (21), and *LMNA* (22). Most recently, mutations were identified in *MIB1* (23) and *RYR2* (24).

In this study, we characterized a large Dutch family presenting with sinus bradycardia in combination with other cardiac abnormalities, including LVNC. In an effort to identify the causal genetic defect underlying this combined phenotypic manifestation in this family, we integrated exome sequencing with linkage analysis, and identified a novel mutation in *HCN4*. *HCN4* encodes the hyperpolarization-activated cyclic nucleotide-gated channel 4, which conducts the hyperpolarization-activated "funny" current (I_f), in the sinoatrial node (SAN) (25,26). In line with the role of this current in SAN pacemaker activity, mutations in *HCN4* have been reported as a cause of sinus bradycardia (2–4). However, the association between *HCN4* mutations and structural cardiac alterations has never been described before. To confirm our results, we subsequently screened *HCN4* in 3 additional families with the same clinical combination of bradycardia and LVNC and have identified *HCN4* mutations in all 3.

METHODS

FAMILY A. In the index family, 7 individuals within 2 generations were affected with bradycardia in combination with LVNC (**Fig. 1**). Available data on medical history, physical examination, 12-lead electrocardiogram (ECG), echocardiography, Holter monitoring, and exercise testing were collected. Genomic deoxyribonucleic acid (DNA) was extracted from peripheral blood according to standard procedures. Written informed consent was obtained from all participating family members.

ECHOCARDIOGRAPHY. Two cardiologists blinded to the described phenotype and to the *HCN4* mutation status analyzed the echocardiographic images. LVNC was called as present or absent by criteria described previously (27,28). Ejection fractions were calculated using the Teichholz M-mode method (**Table 1**).

LINKAGE ANALYSIS. Genome-wide single nucleotide polymorphism (SNP) genotyping was carried out in 5 individuals (II:1, II:3, II:9, III:2, and III:4) from family A, presenting with bradycardia and LVNC using the Illumina HumanOmni2.5 array (Illumina, San Diego, California). Genotypic data were used for linkage analysis to identify chromosomal regions shared among affected individuals. Patient II:6 was excluded from the linkage analysis because at the time of our study, he had persistent atrial fibrillation, and his sinus rhythm could therefore not be assessed (29). Patient II:7 joined the study at a later stage. Linkage analysis was performed using the interface easyLinkage V5.08 (30) running Merlin 1.1.2 (31), with the assumption of an autosomal dominant inheritance pattern, a disease allele frequency of 0.001, and a disease penetrance of 0.9. Mendelian inheritance was checked using PedCheck 1.1 (32). Gene frequency was assumed to be equal between males and females.

have no relationships relevant to the contents of this paper to disclose. Ms. Milano and Dr. Vermeer contributed equally to this work.
Listen to this manuscript's audio summary by *JACC* Editor-in-Chief Dr. Valentin Fuster.
You can also listen to this issue's audio summary by *JACC* Editor-in-Chief Dr. Valentin Fuster.

Manuscript received May 12, 2014; accepted May 21, 2014.

EXOME SEQUENCING. Exome sequencing was carried out on 2 genetically distant family members (cousins III:2 and III:4) at the Beijing Genomics Institute (BGI, Beijing, China). The coding region of the genome was captured using the Agilent SureSelect Target Enrichment system (Agilent Technologies, Santa Clara, California), followed by sequencing on the Illumina HiSeq 2000 platform. The SOAPsnp (for single nucleotide variants) and the GATK (for copy number variants) genome analysis algorithms were used for genotype calling (33,34). Variants were compared using publicly available variant databases—namely: 1) dbSNP132; 2) Exome Variant Server, NHLBI GO Exome Sequencing Project (ESP), Seattle, Washington); 3) Phase 1v3 of the 1,000 Genomes project (data release 10/2012); 4) Genome of the Netherlands (GoNL) (35); and 5) the 69 genomes from Complete Genomics (Mountain View, California)—in addition to 15 in-house exome datasets, using KNIME open-source software version 2.1 with the Knime4Bio plugin (36). Genetic variants found in any of these databases were excluded from further analysis. The 2 exomes were subsequently compared, and genetic variations found in both patients were retained. Variants that remained after filtering were validated by Sanger sequencing and were tested for segregation with the combined (bradycardia-LVNC) phenotype in the family (e.g., testing for presence in all affected and absence in all unaffected family members).

SEQUENCING OF *HCN4* IN ADDITIONAL FAMILIES. The *HCN4* gene (Ensembl Transcript ID ENSG0000013 8622) was screened for coding region mutations in 3 additional families by polymerase chain reaction amplification of the coding regions followed by Sanger sequencing. Primer sequences are available upon request. Segregation analysis of *HCN4* mutations in the families was carried out by Sanger sequencing with the exception of the c.1241C>G in family C, which was done by restriction fragment length polymorphism analysis using HaeII (New England Biolabs, Ipswich, Massachusetts).

MUTATION ANALYSIS OF GENES PREVIOUSLY ASSOCIATED WITH LVNC. The following genes previously associated with LVNC were screened for mutations in the 4 probands (families A through D): *TMP1*, *MYBPC3*, *ACTC1*, *MYH7*, *LDB3*, *DTNA*, *TNNT2*, *TNNI3*, *PLN*, *TAZ*, *LMNA*, *RYR2*, and *MIB1*. The coding region and splice sites of these genes were screened for the presence of novel or rare variants. The *MIB1* gene was screened by polymerase chain reaction-Sanger sequencing. All other genes were screened by next-generation sequencing. For next-generation sequencing, coding exons were captured from 200 ng of genomic DNA using the Agilent HaloPlex Target Enrichment system (Agilent Technologies) following the manufacturer's protocol. Sequencing was carried out on a MiSeq sequencer (Illumina) for 150-bp paired-end read sequencing. Sequence reads were aligned to the human reference genome (standard 1000 Genomes fasta GRCh37 alignment file) using BWA (version 0.6.2) (37) and called using GATK (version 2.6) (34) and SAMtools (version 0.1.19) (38). The mean depth was 171, and 97.8% of the targeted regions were covered at least 10 times. The Knime4Bio tool was used to manage and filter variants (36). Synonymous variations that were not located at splice sites were excluded from further analysis. Heterozygote and homozygote coding and splice site variations of each sequenced patient were compared with publicly available variant databases, namely: 1) dbSNP137, common variant; 2) Phase 1v3 of the 1000 Genomes project (data release 10/2012); 3) NHLBI GO Exome Sequencing Project (ESP, Seattle, Washington); 4) GoNL (35); and 5) the 69 genomes from Complete Genomics.

HAPLOTYPE ANALYSIS IN FAMILIES B AND D. We carried out haplotype analysis to check whether the *HCN4* c.1441T>C mutation in families B and D had a common origin. Ten microsatellite markers flanking *HCN4* were selected (D15S967, D15S981, D15S1050, D15S980, D15S204, D15S211, D15S1041, D15S206, D15S115, and D15S154) and typed in individuals from these families. Primer sequences of all markers were obtained from the UniSTS database. Genomic DNA was amplified in the presence of FAM, and fragments were separated on an ABI3500 genetic analyzer (Applied

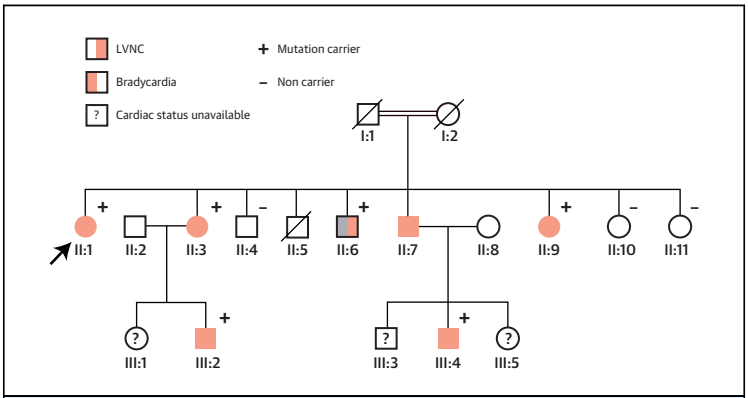

FIGURE 1 Pedigree of Family A

Squares/circles indicate male/female family members, respectively; **open symbols** represent unaffected persons; **symbols with a slash** represent deceased persons; **solid left half**: affected with bradycardia, **solid right half**: left ventricular noncompaction cardiomyopathy (LVNC), **gray**: undetermined. The proband (II:1) is indicated by the **arrow**. HCN4 p.Gly482Arg mutation carriers are indicated by a **plus sign**. The **numbers below the subject symbol** denote the identification of the family members used in the text.

Biosystems, Foster City, California). Results were processed with GeneMapper software 4.1 (Applied Biosystems).

COMPLEMENTARY DNA CONSTRUCTS, MUTAGENESIS, AND HETEROLOGOUS EXPRESSION. The construct (pcDNA3.1) containing wild-type (WT) h*HCN4* complementary DNA (cDNA) was described before (39). The c.1241C>G (p.Ala414Gly) point mutation was introduced into the WT h*HCN4* cDNA by site-directed mutagenesis (QuikChange kit, Stratagene, Agilent Technologies). The *hHCN4* cDNAs containing the mutants c.1441T>C (p.Tyr481His) and c.1444G>C (p.Gly482Arg) were synthesized at Life Technologies (Carlsbad, California) and subsequently cloned into pcDNA3.1.

Chinese hamster ovary (CHO) (Sigma-Aldrich, St. Louis, Missouri) cells were cultured in Ham's F-12 medium with 2 mmol/l glutamine, 10% fetal bovine serum (Lonza, Basel, Switzerland), 1% P/S (5,000 U/ml penicillin and 5,000 U/ml streptomycin sulfate, Lonza) in 5% CO_2 at 37°C. CHO cells were transiently transfected with 2 μg of WT-*HCN4* cDNA or, to recapitulate the heterozygous state, 1 μg of WT and 1 μg of mutant *HCN4* construct, using lipofectamine (Gibco BRL, Life Technologies). Successfully transfected cells were visualized by coexpressed green fluorescent protein (GFP) (0.5 μg eGFP plasmid) (pcDNA3-eGFP, Life Technologies).

WHOLE-CELL-PATCH ELECTROPHYSIOLOGICAL RECORDINGS AND ANALYSIS. HCN4 currents were recorded 2 days after transfection at 37 ± 0.2°C using the amphotericin-perforated patch-clamp technique (Axopatch 200B amplifier, Molecular Devices, Sunnyvale, California). Signals were low-pass filtered (cutoff frequency 5 kHz) and digitized at 5 kHz. Series resistance was compensated by 70% to 80%, and potentials were corrected for the estimated liquid junction potential. Voltage control, data acquisition, and analysis were accomplished using custom software. Superfusion solution contained (in mmol/l): NaCl 140, KCl 5.4, $CaCl_2$ 1.8, $MgCl_2$ 1.0, glucose 5.5, HEPES 5.0 (pH 7.4) (NaOH). Pipettes (borosilicate glass; resistance 2 to 2.5 MΩ) were filled with solution containing (in mmol/l): K-gluc 125, KCl 20, NaCl 10, amphotericin-B 0.88, HEPES 10 (pH 7.2) (KOH). Cell membrane capacitance (7.6 ± 0.6 pF [average ± SEM, n = 35]) was estimated by dividing the decay time constant of the capacitive transient in response to 5 mV hyperpolarizing voltage clamp steps from −20 mV by the series resistance.

HCN4 currents were evoked by hyperpolarizing steps (range −20 to −160 mV, increments of 10 mV) from a holding potential of 0 mV. To prevent membrane instability and cell death at very negative potentials, the duration of the voltage steps was progressively reduced from 12 s (at −20 mV) to 1.5 s (at −160 mV). The voltage step durations were sufficient to reach steady-state activation at all voltages, because activation kinetics of HCN4 channels become faster at more negative potentials (40). Tail currents (at

TABLE 1 Clinical Data of the Families Analyzed in This Study

Patient #	Age (yrs)	Min HR	Max HR	Average HR	Site of Noncompaction*	EF (%)	Medical History†	IVSd	LVIDd	LVPWd	LAEDV
A-II:1	57	31	107	62‡	1, 2	60	OHCA (57 yrs), ICD with pacing capacity	15	46	12	21.6
A-II:3	55	30	103	44	1, 2	64	ICD advised	11	51	8	31.2
A-II:4	54	38	103	63	0	62		11	60	10	24.4
A-II:6	54	48	175	85	1	38	MV reconstruction, maze	10	68	12	71.0
A-II:7	49	NA	NA	NA	1, 2	70	MV reconstruction, maze, OHCA	9	53	10	30.7
A-II:9	47	33	102	46	1, 2	61	Pacemaker	11	46	6	19.1
A-II:10	42	NA	NA	NA	0	51		9	46	8	30.7
A-II:11	45	NA	NA	NA	0	50	OHCA (39 yrs), ICD with pacing capacity	8	60	7	29.3
A-III:2	20	15	126	46	1, 2	50	Pacemaker	11	47	8	17.8
A-III:4	16	26	110	41	1, 2	73	Pacemaker	11	56	12	25.2
B-II:5	54	28	94	50	1, 2	40	AF, myxoid mitral valve, pacemaker	8	54	9	55.0
C-II:4	74	32	169	66	1, 2	30	AF, ICD with pacing capacity	9	49	13	26.9
C-III:1	44	NA	NA	NA	1	70	LV hypertrophy (IVS = 13 mm)	13	NA	13	23.3
C-III:2	42	30	111	55	1, 2	70	LV hypertrophy (IVS = 13 mm)	13	55	11	35.1
D-II:4	NA	NA	NA	NA	NA	NA	Pacemaker	NA	NA	NA	NA
D-III:2	36	27	92	44	1, 2	41	Pacemaker	11	75	11	22.1

*Numbering for the site of noncompaction: none = 0, left ventricular apex = 1, right ventricular involvement = 2. †The number in parentheses indicates the patient's age in years at the time of OHCA. ‡Holter report shows extreme bradycardia.

AF = atrial fibrillation; EF = ejection fraction; HR = heart rate; ICD = implantable cardioverter defibrillator; IVS = interventricular septum; IVSd = interventricular septum in diastole; LV = left ventricular; LAEDV = left atrial end diastolic volume indexed for body surface area; LVIDd = left ventricular internal diastolic dimension; LVPWd = left ventricular posterior wall in diastole; MV = mitral valve; NA = not assessed; OHCA = out-of-hospital cardiac arrest.

0 mV), plotted against test voltage, provided the activation-voltage relationship; the latter was normalized by maximum amplitude and fitted with the Boltzmann function: $I/I_{max} = A/\{1.0 + \exp[(V-V_{1/2})/k]\}$ to determine the half-maximum activation voltage ($V_{1/2}$) and slope factor (k).

STATISTICAL ANALYSIS. Data are mean ± SEM. Groups were compared using 1-way analysis of variance followed by Tukey's test or 2-way repeated measures analysis of variance followed by pairwise comparison using the Student-Newman-Keuls test. A p value of <0.05 defined statistical significance.

RESULTS

FAMILY A. The pedigree of the index family is shown in Figure 1. The proband (II:1) visited our cardiogenetics outpatient clinic because of an out-of-hospital cardiac arrest (OHCA) as a result of ventricular fibrillation at the age of 57 and a positive family history for cardiomyopathy. A previously made Holter recording showed episodes of bradycardia for 7% of the 24 h, with a minimum heart rate of 31 beats/min. Further evaluation initially did not reveal any abnormalities, and an implantable cardioverter-defibrillator (ICD) (with pacing capacity) was implanted for secondary prevention of sudden cardiac death. LVNC of the myocardium was detected after evaluation of her echocardiographs.

Three siblings (II:3, II:7, and II:9) and 2 nephews (III:2 and III:4) of the proband presented with the same combination of bradycardia and LVNC. Anamnestically, the sinus bradycardia of III:2 was first detected in utero during Doppler echocardiographic evaluation. A pacemaker was implanted in II:7, II:9, and III:2, because of bradycardia-related symptoms. Clinical data of family A are presented in Table 1.

Two individuals (II:6 and II:7) had mitral valve reconstruction because of a mitral valve prolapse. Post-operative atrial fibrillation occurred in II:6, and he was unsuccessfully treated by a surgical maze procedure; consequently, we could not determine the occurrence of bradycardia in this individual (29). His echocardiogram showed LVNC. In 2013, II:7 collapsed during breakfast; he regained consciousness after 1 to 2 min and was admitted to the hospital. The ECG record showed atrial fibrillation. Later, a sinus rhythm with a total atrioventricular block, without an adequate escape rhythm, was observed. Given his LVNC, worsening systolic function with signs of progressive conduction disorders, and the expectation of frequent pacing, his pacemaker was replaced by a biventricular ICD. Cardiac evaluation of II:4 and II:10 did not reveal any abnormalities.

TABLE 2 Overview of Known Human *HCN4* Mutations

Residue Change	HCN4 Domain Position	Patients' Clinical Characteristics	HCN4 Domain (Ref. #)
p.Ala195Val	Cytoplasmic	Sinus bradycardia in sudden infant death syndrome	(51)
p.Gly482Arg	Pore	Family A	This study
p.Tyr481His	Pore	Families B and D	This study
p.Ala414Gly	S4–S5 linker	Family C	This study
p.Ile404fs	Extracellular S5-pore	ST-segment elevation and complete right bundle branch block	(52)
p.Gly480Arg	Pore	Sinus bradycardia	(4)
p.Ala485Val	Pore	Sinus bradycardia	(3)
p.Lys530Asn	C-linker	Tachycardia-bradycardia syndrome and AF	(53)
p.Asp553Asn	C-linker	Sinus bradycardia with torsade de pointes ventricular tachycardia	(54)
p.Pro544fs	C-linker	Sinus bradycardia	(6)
p.Ser672Arg	cAMP binding domain	Sinus bradycardia	(55)
p.Thr644fs	cAMP binding domain	Sinus bradycardia with premature beats linked to adrenergic stress	(56)
p.Val759Ile	Cytoplasmic	Sinus bradycardia in sudden infant death syndrome	(51)

AF = atrial fibrillation; cAMP = cyclic adenosine monophosphate.

The youngest sister of the proband (II:11) had an OHCA at 39 years old as a result of ventricular fibrillation. During her hospital admission, she was repeatedly defibrillated because of sustained polymorphic ventricular tachycardias, initiated by short-coupled ventricular extrasystole. After an electrophysiology study, in which a right bundle branch block morphology with extreme axis focus was ablated, no further arrhythmias were observed. Echocardiographic investigation did not reveal signs of cardiomyopathy. The parents of the proband, who were distantly related (seventh-degree relatives), are deceased, and no clinical information was available.

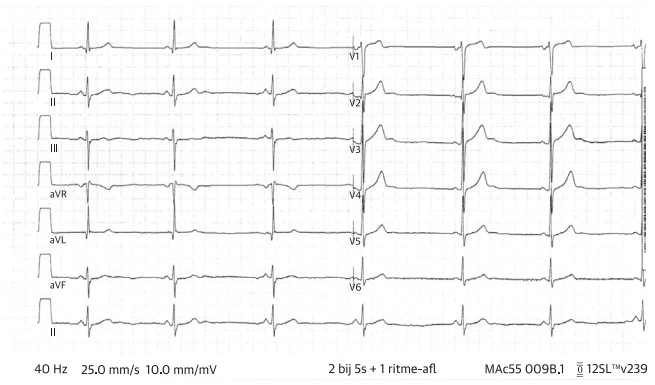

FIGURE 2 Typical ECG Showing the Bradycardia in Family A

The electrocardiogram (ECG) is from a Holter recording of III:2, family A.

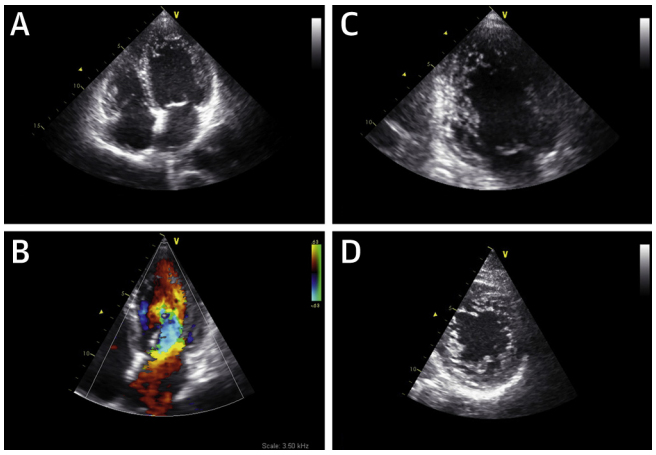

FIGURE 3 Echocardiographic Image of An Affected Individual (III:4) With LVNC and Bradycardia

End-systolic apical 4-chamber view shows left ventricular noncompaction cardiomyopathy (LVNC) **(A)**, apical 4-chamber view with color Doppler image shows deep recesses filled with blood from the left ventricular cavity at end-diastole **(B)**, apical 2-chamber view **(C)**, and short-axis view **(D)**. Note the widespread prominent left ventricular trabeculations and deep intertrabecular recesses extending into the mid-ventricular portion of the inferior wall in the affected patient. See accompanying Online Videos 1, 2, and 3.

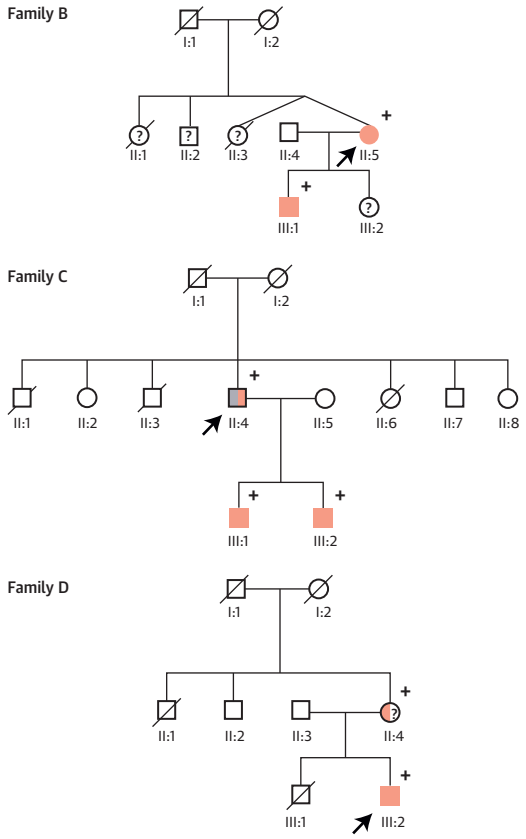

FIGURE 4 Additional Families With Sinus Bradycardia and LVNC

HCN4 mutation carriers are indicated by a +: p.Tyr481His in family B and D, p.Ala414Gly in family C. Description of symbols as in Figure 1. LVNC = left ventricular noncompaction cardiomyopathy.

Representative ECG traces are presented in Figure 2 (III:4). Representative echocardiographic findings of an affected family member (III:4) are presented in Figure 3 and Online Videos 1, 2, and 3.

GENOME-WIDE LINKAGE ANALYSIS. We set out to identify the genetic defect underlying the combined phenotype of bradycardia and LVNC. Although the parents are distantly related, the pedigree of family A is suggestive of an autosomal dominant pattern of inheritance. Linkage analysis in 5 relatives with combined bradycardia and LVNC was performed. All loci with suggestive linkages were checked for sharing in all 5 individuals by haplotype analysis; we thus uncovered 30 loci that were shared among all affected individuals (Online Fig. 1). In total, these shared regions span ~492 Mb and contain >2,000 coding genes.

EXOME SEQUENCING. Exome sequencing was carried out on cousins III:2 and III:4 in family A. Coverage and quality scores of the exome sequencing experiment are shown in Online Table 1. The number of exonic variants identified per sequenced individual is shown in Online Table 2. We identified 72 novel shared variants not previously reported in public variant databases, including the ethnically matched GoNL study (35). We overlaid these variants with the 30 linkage regions, thus narrowing the list down to 11 novel shared variants (Online Table 3). Of these, only 1 variant in *HCN4* (c.1444G>C, p.Gly482Arg) cosegregated with the combined phenotype in the remaining affected family members and was absent in all unaffected family members. Subject II-6, who had LVNC, but in whom the presence of sinus bradycardia could not be evaluated, carried the mutation.

ADDITIONAL FAMILIES: PEDIGREES. To further explore the possible link between mutations in *HCN4* and the combined phenotype of bradycardia and LVNC, we screened *HCN4* in 3 additional families with this combined clinical presentation. The pedigree of families B, C, and D are shown in Figure 4.

FAMILY B. The proband of family B (individual II:5) was referred to the cardiologist after she collapsed in the shower. The cardiovascular examination

revealed bradycardia, LVNC, and a myxoid degeneration of the mitral valve. Moreover, polymorphic ventricular extrasystoles occurred during exercise. A few months later, she presented with atrial fibrillation at age 53 years. A loop recorder showed more than 800 episodes of bradycardia in 64 days (heart rate <30 beats/min). Because of the syncope and the frequent episodes of bradycardia, a pacemaker was implanted. Her son also presented with the combined phenotype. Both were carriers of a mutation in *HCN4* (c.1441T>C, p.Tyr481His).

FAMILY C. The proband of family C (individual II:4) is a 74-year-old man who presented with atrial fibrillation; echocardiographic evaluation revealed LVNC. His 2 sons, presented with the combined phenotype of LVNC and bradycardia. On Holter monitoring, 1 displayed severe sinus bradycardia involving 12 episodes of standstill with a maximum duration of 2.88 s, which most of the time occurred during episodes of bradyarrhythmia. All 3 carried a mutation in *HCN4* (c.1241C>G, p.Ala414Gly).

FAMILY D. The proband of family D (individual III:2) has been previously described in a case report (10). A 36-year-old man was referred because of progressive fatigue. Cardiovascular examination revealed a severe sinus bradycardia (40 beats/min), LVNC, and moderate aortic valve regurgitation. His mother (D:II:4) has a pacemaker because of bradyarrhythmias. Echocardiographic reports of the mother were not available. The *HCN4* mutation (c.1441T>C, p.Tyr481His) that was found in family B was identified in the proband and his mother.

To determine whether the c.1441T>C mutation of families B and D had a common origin, we investigated the haplotype harboring this mutation in the 2 families. This provided evidence of a common ancestral haplotype (Fig. 5).

None of the mutations identified in this study were found in large sets of the general population, including 6,503 individuals from the Exome Variation Database NHLBI GO Exome Sequencing Project (ESP, Seattle, Washington) and 500 ethnically matched (Dutch) controls from the GoNL project. The 3 *HCN4* mutations identified in this study are presented in Figure 6. They affect residues fully conserved among 98 species from lamprey to human (data not shown).

ADDITIONAL GENETIC ANALYSIS. To ensure that the LVNC phenotype in families A through D was not due to mutations in any of the known LVNC genes, the probands from these families were screened for mutations in these genes. No novel or rare (minor allele frequency <1%) mutations in the known LVNC genes were found.

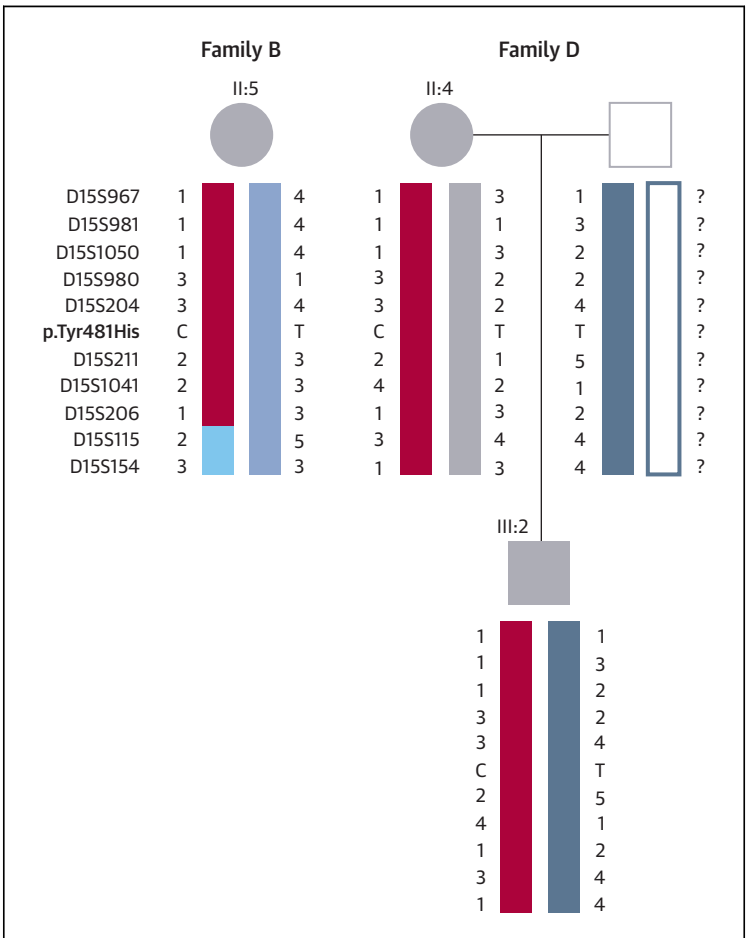

FIGURE 5 Haplotype Analysis of 10 Microsatellite Markers at the HCN4 Locus in Families B and D, With the p.Tyr481His Mutation in *HCN4*

The haplotype containing the *HCN4* mutation is colored **red**. Markers D15S206 and D15S115 flanking the recombination event telomeric of the mutation are 200 kB apart.

ELECTROPHYSIOLOGY OF MUTANT HCN4 CHANNELS. WT and mutant HCN4 channels were transiently expressed in CHO cells, and the biophysical properties were examined using the voltage clamp protocol as depicted in Figure 7A, top panel. Tail currents (Fig. 7A, bottom, inset) were used to analyze the voltage dependence of activation (Fig. 7B, left panel). Half-maximal activation voltages ($V_{1/2}$) in all mutant HCN4 channels were significantly more negative as compared with WT channels, whereas no differences in slope factor (k) were observed (Fig. 7B, right panels). The current density at −160 mV, the potential at which all groups in all channels are activated (Fig. 7B, left panel), did not differ significantly, although there is a tendency to smaller densities (Fig. 7C, left panel) (−184 ± 35 pA/pF [WT, n = 11], −120 ± 30 pA/pF [WT+p.Ala414Gly, n = 9], −100 ± 18 pA/pF [WT+p.Tyr481His, n = 8], and −97 ± 21 pA/pF

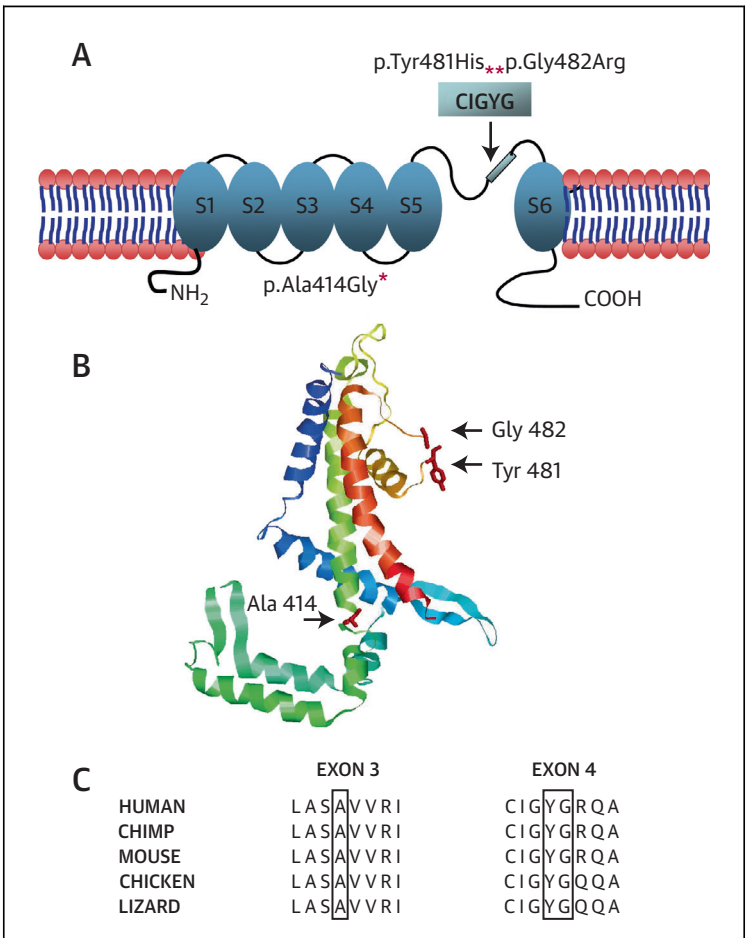

FIGURE 6 Overview of the Protein Changes in *HCN4*

(A) Schematic diagram of the *HCN4* mutation locations with respect to the channel domains. **(B)** Structural model of HCN4 channel obtained from a ribbon SwissProt model of amino acids 264–520. Positions of the mutated amino acids are indicated by hydrogen bonds. **Arrows** show the locations of the novel *HCN4* mutations identified in this study. **(C)** p.Ala414Gly, p.Tyr481His, and p.Gly482Arg are evolutionary conserved amino acid residues.

[WT+p.Gly482Arg, n = 7]). However, as a consequence of the shifts in voltage dependence of activation, the current density of all mutant HCN4 channels was significantly lower, at −60 mV and −50 mV (**Fig. 7C**, right panels), for example, in the voltage range of diastolic depolarization of human SAN pacemaker cells (**Figs. 7B and 7C**, gray area) (25). The lower current densities of the mutant HCN4 channels in the voltage range of human SAN diastolic depolarization are consistent with the bradycardia observed in the patients.

DISCUSSION

For the first time, we provide strong evidence linking mutations in *HCN4* to the combined clinical presentation of bradycardia and LVNC. Using a strategy entailing linkage analysis and exome sequencing, we first identified the causal *HCN4* mutation in a large pedigree with individuals affected by the combined phenotype. Follow-up screening of *HCN4* in 3 other families with the same combined clinical presentation uncovered 2 additional *HCN4* mutations in the 3 families. Although mutations in *HCN4* have been previously linked to bradycardia (**Table 2**), our study provides the first evidence to our knowledge that mutations in this ion channel gene also may be associated with structural abnormalities of the myocardium.

HCN4 encodes the fourth isoform of the hyperpolarization-activated cyclic nucleotide-gated channel 4, which conducts the hyperpolarization-activated "funny" current, among others in the SAN (25,26). In line with the role of this current in SAN pacemaker activity, the *HCN4* locus has been identified as a modulator of heart rate in a recent genome-wide association study (41), and mutations in *HCN4* have been reported as a cause of sinus bradycardia (2–4). None of these studies, however, describe structural cardiac alterations, although it is unclear whether patients involved were actively screened for this.

The HCN4 channel is composed of 6 transmembrane domains and a pore-forming loop—the P domain—located between transmembrane domains S5 and S6, acting as the ion conducting pore and selectivity filter (40). Two of the identified mutations, p.Tyr481His and p.Gly482Arg, affect highly conserved residues within this channel domain (**Fig. 6**). Our heterologous expression studies of WT HCN4 with mutant HCN4 carrying, respectively, the p.Tyr481His and the p.Gly482Arg mutations (reflecting the heterozygous situation in mutation carriers), uncovered a large negative shift of the voltage dependence of activation compared with the expression of only WT channels. This finding is in agreement with previous observations for 2 other pore-region *HCN4* mutations, namely p.Gly480Arg (4) and p.Ala485Val (3), both located close to p.Tyr481His and p.Gly482Arg, indicating the importance of the pore region of the channel for the voltage dependence of activation. The other mutation we identified, p.Ala414Gly, which is also evolutionarily highly conserved, is the first mutation described in the S4-S5 linker. The cytoplasmic S4-S5 linker of HCN channels is thought to play a role in voltage-activated gating (42). Consistent with this hypothesis, p.Ala414Gly resulted in a negative shift of the voltage dependence of activation. The shifts of the activation voltage dependence toward more negative

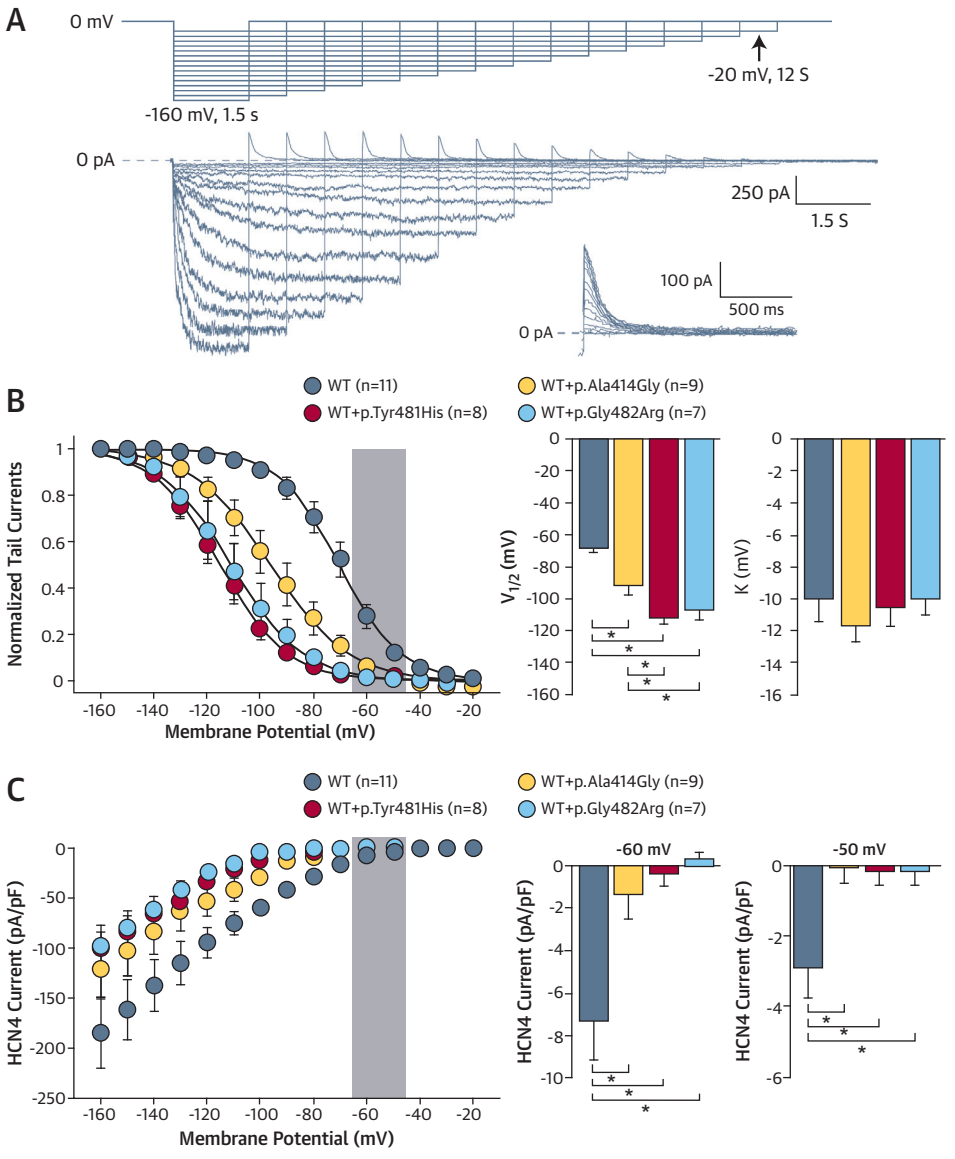

FIGURE 7 ***HCN4*** **Mutations Shift the Voltage Dependency of Activation Towards More Negative Potentials**

(A) Voltage clamp protocol **(top panel)** and typical wild-type (WT) HCN4 current **(bottom panel)**. **Inset**, superimposed tail currents. **(B)** Voltage dependency of activation **(left panel)**. The **dashed curves** are the Boltzmann fits to the data, and the **gray area** represents the voltage range of diastolic depolarization of human sinoatrial node (SAN) pacemaker cells. Average half-maximum activation voltage ($V_{1/2}$) and slope factor (k) **(right panels)**. Note that the mutant channels activate at more negative potentials (−68.4 ± 2.8, −92.3 ± 5.3, −112.3 ± 3.5, and −107.1 ± 6.1 for WT [n = 11], WT+p.Ala414Gly [n = 9], WT+p.Tyr481His [n = 8], and WT+p.Gly482Arg [n = 7], respectively). **(C)** Current-voltage relationships of WT and mutant HCN4 channels **(left panel)**. The **gray area** represents the voltage range of diastolic depolarization of human SAN pacemaker cells. Average current density at −60 and −50 mV **(right panels)**. Note that current densities in mutant channels are significantly smaller compared with WT HCN4.

potentials observed for the 3 mutations result in a significantly lower HCN4 current density in the potential range of the diastolic depolarization (i.e., the action potential phase responsible for the spontaneous activity of SAN cells). The very small inward current that drives the diastolic depolarization is the net result of a complex interaction of a large number of inward and outward currents, including the inwardly directed HCN4-mediated current underlying I_f (40). The reduced I_f observed for the 3 mutations is

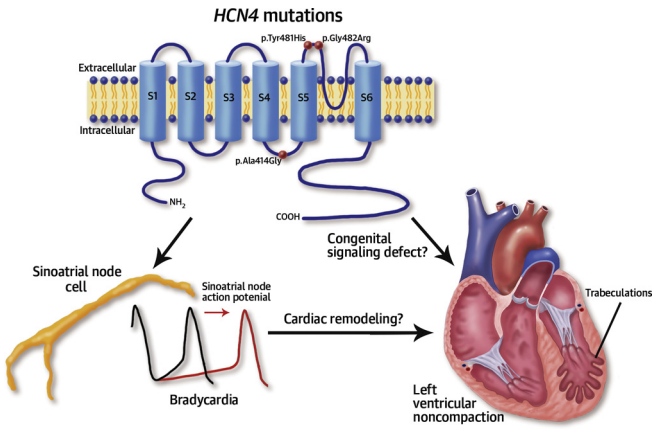

CENTRAL ILLUSTRATION ***HCN4* Mutations in Bradycardia and LVNC**

Location of *HCN4* mutations causing the combined clinical presentation of bradycardia and left ventricular noncompaction (LVNC). The 3 mutations decrease HCN4 current density in the potential range of the diastolic depolarization in sinoatrial cells causing the bradycardia. The mechanism underlying the LVNC remains unknown. We hypothesize that LVNC as a result of mutation in the *HCN4* gene may arise from a congenital signaling defect or could occur as a consequence of cardiac remodeling in response to the lower heart rate.

thus compatible with the clinically observed bradycardia.

Although the involvement of *HCN4* mutations in bradycardia is in line with the established role of *HCN4* in cardiac pacing, the mechanism underlying the LVNC observed in the described families is unclear. We formed 2 possible hypotheses that will require further testing (**Central Illustration**):

1. LVNC may be congenital and the direct result of the *HCN4* mutations in these families. In humans, the trabecular myocardium compacts around 8 weeks of gestation, following ventricular septation (43). In mice, at this developmental stage, *Hcn4* is expressed within the SAN (44) and in humans also is detectable in the trabecular (subendocardial) layer, although at a low level in comparison with that of the SAN (45). Furthermore, a recent study demonstrated that *Hcn4* is expressed in an early progenitor pool of cells that ultimately gives rise to the left ventricle (both compact and trabecular) (46). The presence of *HCN4* in precursors of the ventricular wall myocardium would allow for a signaling function of *HCN4* in the process of normal compaction of the human fetal ventricles.
2. A second hypothesis may be that the observed LVNC is an acquired feature in response to sinus bradycardia, as an adaptive remodeling to enable increased stroke volume and improved cardiac oxygen uptake. This hypothesis is supported by the fact that mild trabeculations are a physiological response to exercise (47). Possible future studies could entail longitudinal studies in patients taking the I_f-blocker ivabradine—a common angina pectoris medication for which bradycardia is a common side effect—to check the possible development of LVNC.

The possibility that LVNC may be an incidental finding seems unlikely, given the very low frequency in the population (0.05%) (48) and the consistent observation of this feature in all the *HCN4* mutation carriers across all families, whereas it was absent in the noncarriers. This study will further aid the diagnostic challenges associated with LVNC. Other cardiac complications are present in the families, including myxoid mitral valve, atrial fibrillation, left ventricular hypertrophy, and sudden cardiac arrest. The latter occurred in 2 individuals from family A, one with and the other without the familial *HCN4* mutation. The occurrence of OHCA in the individual who tested negative for the familial *HCN4* mutation could point to an additional genetic defect in the family. Screening of a large panel of genes associated with primary electrical disease or cardiomyopathy in this individual, however, did not identify any putative mutation (data not shown).

Cardiac ion channel mutations thus far have been mainly identified in association with arrhythmic disorders of the heart, attributed to primary arrhythmia syndromes without myocardial abnormalities. However, in line with the findings presented in this study, evidence is now accumulating that primary channelopathies also can be associated with the development of myocardial structural abnormalities (49,50).

STUDY LIMITATIONS. In this study, although the genetic evidence for the involvement of the *HCN4* mutations in the combined bradycardia-LVNC phenotype is very strong, and the electrophysiological data provide strong evidence for causality of the *HCN4* mutations in the pathogenesis of the observed bradycardia, the mechanism whereby *HCN4* mutations lead to LVNC remains unknown.

CONCLUSIONS

For the first time, we link mutations in *HCN4* to a combined phenotype of bradycardia and LVNC. Our findings implicate mutations in this ion channel gene in cardiac structural abnormalities in addition to sinus bradycardia.

ACKNOWLEDGMENTS The authors thank M.R. Lombardi and M. Klerk for their technical assistance, and Dr. Sabine Klaassen for insightful discussions. The authors also thank Berend de Jonge and the Genomics Core Facility of Nantes (Biogenouest Genomics) for technical support.

REPRINT REQUESTS AND CORRESPONDENCE: Dr. Connie R. Bezzina, Department of Clinical and Experimental Cardiology, Academic Medical Center, Meibergdreef 9, 1105 AZ Amsterdam, the Netherlands. E-mail: c.r.bezzina@amc.uva.nl.

PERSPECTIVES

COMPETENCY IN MEDICAL KNOWLEDGE: The combined cardiac phenotype of sinus bradycardia in association with left ventricular noncompaction cardiomyopathy (LVNC) is now linked to mutations in *HCN4* in multiple families.

TRANSLATIONAL OUTLOOK 1: Although the pathogenetic mechanism whereby *HCN4* mutations cause bradycardia is established, additional research is needed to uncover the mechanism by which such mutations cause LVNC.

REFERENCES

1. Monfredi O, Dobrzynski H, Mondal T, Boyett MR, Morris GM. The anatomy and physiology of the sinoatrial node—a contemporary review. Pacing Clin Electrophysiol 2010;33:1392–406.

2. Milanesi R, Baruscotti M, Gnecchi-Ruscone T, DiFrancesco D. Familial sinus bradycardia associated with a mutation in the cardiac pacemaker channel. New Engl J Med 2006;354:151–7.

3. Laish-Farkash A, Glikson M, Brass D, et al. A novel mutation in the HCN4 gene causes symptomatic sinus bradycardia in Moroccan Jews. J Cardiovasc Electrophysiol 2010;21:1365–72.

4. Nof E, Luria D, Brass D, et al. Point mutation in the HCN4 cardiac ion channel pore affecting synthesis, trafficking, and functional expression is associated with familial asymptomatic sinus bradycardia. Circulation 2007;116:463–70.

5. Benson DW, Wang DW, Dyment M, et al. Congenital sick sinus syndrome caused by recessive mutations in the cardiac sodium channel gene SCN5A. J Clin Invest 2003;112:1019–28.

6. Smits JPP, Koopmann TT, Wilders R, et al. A mutation in the human cardiac sodium channel (E161K) contributes to sick sinus syndrome, conduction disease and Brugada syndrome in two families. J Mol Cell Cardiol 2005;38:969–81.

7. Le Scouarnec S, Bhasin N, Vieyres C, et al. Dysfunction in ankyrin-B-dependent ion channel and transporter targeting causes human sinus node disease. Proc Natl Acad Sci U S A 2008;105:15617–22.

8. Caliskan K, Balk AHMM, Jordaens L, Szili-Torok T. Bradycardiomyopathy: the case for a causative relationship between severe sinus bradycardia and heart failure. J Cardiovasc Electrophysiol 2010;21:822–4.

9. Ozkutlu S, Onderoglu L, Karagöz T, Celiker A, Sahiner UM. Isolated noncompaction of left ventricular myocardium with fetal sustained bradycardia due to sick sinus syndrome. Turk J Pediatr 2006;48:383–6.

10. Dellefave LM, Pytel P, Mewborn S, et al. Sarcomere mutations in cardiomyopathy with left ventricular hypertrabeculation. Circ Cardiovasc Genet 2009;2:442–9.

11. Egan KR, Ralphe JC, Weinhaus L, Maginot KR. Just sinus bradycardia or something more serious? Case Rep Pediatr 2013;2013:1–5.

12. Chin TK, Perloff JK, Williams RG, et al. Isolated noncompaction of left ventricular myocardium. A study of eight cases. Circulation 1990;82:507–13.

13. Oechslin E, Jenni R. Left ventricular noncompaction revisited: a distinct phenotype with genetic heterogeneity? Eur Heart J 2011;32:1446–56.

14. Sugiyama H, Hoshiai M, Toda T, Nakazawa S. Double-orifice mitral valve associated with noncompaction of left ventricular myocardium. Pediatr Cardiol 2006;27:746–9.

15. Klaassen S, Probst S, Oechslin E, et al. Mutations in sarcomere protein genes in left ventricular noncompaction. Circulation 2008;117:2893–901.

16. Hoedemaekers YM, Caliskan K, Majoor-Krakauer D, et al. Cardiac beta-myosin heavy chain defects in two families with non-compaction cardiomyopathy: linking non-compaction to hypertrophic, restrictive, and dilated cardiomyopathies. Eur Heart J 2007;28:2732–7.

17. Monserrat L, Hermida-Prieto M, Fernandez X, et al. Mutation in the alpha-cardiac actin gene associated with apical hypertrophic cardiomyopathy, left ventricular non-compaction, and septal defects. Eur Heart J 2007;28:1953–61.

18. Bleyl SB, Mumford BR, Thompson V, et al. Neonatal, lethal noncompaction of the left ventricular myocardium is allelic with Barth syndrome. Am J Hum Genet 1997;61:868–72.

19. Ichida F, Tsubata S, Bowles KR, et al. Novel gene mutations in patients with left ventricular noncompaction or Barth syndrome. Circulation 2001;103:1256–63.

20. Vatta M, Mohapatra B, Jimenez S, et al. Mutations in Cypher/ZASP in patients with dilated cardiomyopathy and left ventricular noncompaction. J Am Coll Cardiol 2003;42:2014–27.

21. Hoedemaekers YM, Caliskan K, Michels M, et al. The importance of genetic counseling, DNA diagnostics, and cardiologic family screening in left ventricular noncompaction cardiomyopathy. Circ Cardiovasc Genet 2010;3:232–9.

22. Hermida-Prieto M, Monserrat L, Castro-Beiras A, et al. Familial dilated cardiomyopathy and isolated left ventricular noncompaction associated with lamin A/C gene mutations. Am J Cardiol 2004;94:50–4.

23. Luxán G, Casanova JC, Martínez-Poveda B, et al. Mutations in the NOTCH pathway regulator MIB1 cause left ventricular noncompaction cardiomyopathy. Nat Med 2013;19:193–201.

24. Ohno S, Omura M, Kawamura M, et al. Exon 3 deletion of RYR2 encoding cardiac ryanodine receptor is associated with left ventricular noncompaction. Europace 2014;16:1–9.

25. Verkerk AO, Wilders R, Van Borren MMGJ, et al. Pacemaker current (If) in the human sinoatrial node. Eur Heart J 2007;28:2472–8.

26. Xu X, Vysotskaya ZV, Liu Q, Zhou L. Structural basis for the cAMP-dependent gating in the human HCN4 channel. J Biol Chem 2010;285:37082–91.

27. Sasse-Klaassen S, Probst S, Gerull B, et al. Novel gene locus for autosomal dominant left ventricular noncompaction maps to chromosome 11p15. Circulation 2004;109:2720–3.

28. Jenni R, Oechslin E, Schneider J, et al. Echocardiographic and pathoanatomical characteristics of isolated left ventricular non-compaction: a step towards classification as a distinct cardiomyopathy. Heart 2001;86:666–71.

29. Mangrum J, DiMarco JP. The evaluation and management of bradycardia. N Engl J Med 2000;342:703–9.

30. Hoffmann K, Lindner TH. easyLINKAGE-Plus—automated linkage analyses using large-scale SNP data. Bioinformatics 2005;21:3565–7.

31. Abecasis GR, Cherny SS, Cookson WO, Cardon LR. Merlin—rapid analysis of dense genetic maps using sparse gene flow trees. Nat Genet 2002;30:97–101.

32. O'Connell JR, Weeks DE. PedCheck: a program for identification of genotype incompatibilities in linkage analysis. Am J Hum Genet 1998;63:259–66.

33. Li R, Yu C, Li Y, et al. SOAP2: an improved ultrafast tool for short read alignment. Bioinformatics 2009;25:1966–7.

34. McKenna A, Hanna M, Banks E, et al. The genome analysis toolkit: a mapReduce framework for analyzing next-generation DNA sequencing data. Genome Res 2010;20:1297–303.

35. Boomsma DI, Wijmenga C, Slagboom EP, et al. The Genome of the Netherlands: design, and project goals. Eur J Hum Genet 2014;22:221–7.

36. Lindenbaum P, Le Scouarnec S, Portero V, Redon R. Knime4Bio: a set of custom nodes for the interpretation of next-generation sequencing data with KNIME. Bioinformatics 2011;27:3200–1.

37. Li H, Durbin R. Fast and accurate short read alignment with Burrows-Wheeler transform. Bioinformatics 2009;25:1754–60.

38. Li H, Handsaker B, Wysoker A, et al. The sequence alignment/map format and SAMtools. Bioinformatics 2009;25:2078–9.

39. Boink GJJ, Verkerk AO, Van Amersfoorth SCM, et al. Engineering physiologically controlled pacemaker cells with lentiviral HCN4 gene transfer. J Gene Med 2008;10:487–97.

40. Verkerk AO, Van Ginneken ACG, Wilders R. Pacemaker activity of the human sinoatrial node: role of the hyperpolarization-activated current, If. Int J Cardiol 2009;132:318–36.

41. den Hoed M, Eijgelsheim M, Esko T, et al. Identification of heart rate-associated loci and their effects on cardiac conduction and rhythm disorders. Nat Genet 2013;45:621–34.

42. Chen J, Mitcheson JS, Tristani-Firouzi M, Lin M, Sanguinetti MC. The S4-S5 linker couples voltage sensing and activation of pacemaker channels. Proc Natl Acad Sci U S A 2001;98:11277–82.

43. Sedmera D, Pexieder T, Vuillemin M, Thompson RP, Anderson RH. Developmental patterning of the myocardium. Anat Rec 2000;258:319–37.

44. Garcia-Frigola C, Shi Y, Evans SM. Expression of the hyperpolarization-activated cyclic nucleotide-gated cation channel HCN4 during mouse heart development. Gene Expr Patterns 2003;3:777–83.

45. Sizarov A, Devalla HD, Anderson RH, Passier R, Christoffels VM, Moorman AF. Molecular analysis of patterning of conduction tissues in the developing human heart. Circ Arrhythm Electrophysiol 2011;4:532–42.

46. Später D, Abramczuk MK, Buac K, et al. A HCN4+ cardiomyogenic progenitor derived from the first heart field and human pluripotent stem cells. Nat Cell Biol 2013;15:1098–106.

47. Estes NA III, Link MS, Cannom D, et al. Report of the NASPE policy conference on arrhythmias and the athlete. J Cardiovasc Electrophysiol 2001;12:1208–19.

48. Jenni R. Isolated noncompaction of the myocardium. N Engl J Med 1999;340:966–7.

49. Olson TM, Michels VV, Ballew JD, et al. Sodium channel mutations and susceptibility to heart failure and atrial fibrillation. JAMA 2005;293:447–54.

50. McNair WP, Ku L, Taylor MRG, et al. SCN5A mutation associated with dilated cardiomyopathy, conduction disorder, and arrhythmia. Circulation 2004;110:2163–7.

51. Evans A, Bagnall RD, Duflou J, Semsarian C. Postmortem review and genetic analysis in sudden infant death syndrome: an 11-year review. Hum Pathol 2013;44:1730–6.

52. Ueda K, Hirano Y, Higashiuesato Y, et al. Role of HCN4 channel in preventing ventricular arrhythmia. J Hum Genet 2009;54:115–21.

53. Duhme N, Schweizer PA, Thomas D, et al. Altered HCN4 channel C-linker interaction is associated with familial tachycardia-bradycardia syndrome and atrial fibrillation. Eur Heart J 2013;34:2768–75.

54. Netter MF, Zuzarte M, Schlichthörl G, Klöcker N, Decher N. The HCN4 channel mutation D553N associated with bradycardia has a C-linker mediated gating defect. Cell Physiol Biochem 2012;30:1227–40.

55. Xu X, Marni F, Wu S, et al. Local and global interpretations of a disease-causing mutation near the ligand entry path in hyperpolarization-activated cAMP-gated channel. Structure 2012;20:2116–23.

56. Schweizer PA, Duhme N, Thomas D, et al. cAMP sensitivity of HCN pacemaker channels determines basal heart rate but is not critical for autonomic rate control. Circ Arrhythm Electrophysiol 2010;3:542–52.

KEY WORDS exome sequencing, genetics, *HCN4*, ion channel, left ventricular noncompaction cardiomyopathy, sinus bradycardia

APPENDIX For supplemental tables, videos, and a figure, please see the online version of this article.